Expanded method section, tables and additional figures

Item DR1: Sample Analysis

The analysis process involveed four key stages; pre-concentration of ^{234}U and ^{230}Th, separation of ^{234}U and ^{230}Th, analysis of samples using mass spectroscopy and processing of results for age calculation. All stages of the analytical procedure were carried out at the Scottish Universities Environmental Research Centre (SUERC). Selected samples were ground to <200 mesh and well mixed before aliquots were taken for analysis. Complete dissolution of samples was achieved by nitric acid digestion. Samples were spiked with a mixed ^{229}Th - ^{236}U tracer. U and Th were isolated from the aliquots using the first stage of the column separation method described by Yokoyama et al. (1999). Matrix elements of the sample were eluted with 4 M HNO_3, Th eluted with 5 M HCl and U with 0.1 M HNO_3. 5M HCl was used to prevent the carry-over of Th into the U fraction and optimise U-Th separation. After separation the U faction was diluted with 5% (v/v) HNO_3 in order to achieve an appropriate concentration of U (~50 ppb) for analysis. Th samples were taken up in a 50 ppb solution of the certified reference material (CRM) NBL112-A (natural U) which was used to monitor and correct instrumental mass bias.

Analysis of samples was carried out on an upgraded Micromass Isoprobe MC-ICP-MS equipped with 9 Faraday collectors and an ion counting Daly-photo-multiplier detector located behind a wide-access retarding potential (WARP) filter. An Elemental Scientific Inc. Apex nebuliser system equipped with heating, cooling and decolvation stages was used to introduce samples to the ICP-MS. For ^{234}U analysis a 2-cycle measurement was employed. In the first cycle ^{234}U was analysed using the Daly detector (typically 5000 cps) while ^{235}U, ^{236}U (spike), and ^{238}U were measured simultaneously using Faraday detectors. In cycle 2, ^{235}U was measured on the Daly detector and ^{238}U was measured on a Faraday. The two ^{238}U measurements were used to correct for any fluctuation in ion beam intensity while the ^{235}U measurements were used to quantify the relative gains of Daly and Faraday detectors (nominally 97% and stable to less than 0.1% over several hours). Measured ^{235}U/^{238}U was used to correct instrumental mass bias assuming a natural ratio and an exponential law. Th analysis was also carried out with a 2 cycle routine with ^{229}Th spiked to an appropriate level to allow detection on both Daly and Faraday detectors. In cycle 1 ^{229}Th was measured on the Daly and ^{235}U and ^{238}U were measured on Faradays and used to correct mass bias using an exponential law and the certified natural ratio of NBL112-A. In cycle 2 ^{229}Th was measured on a Faraday and used to calculate the relative Daly-Faraday gain (typically about 0.5% lower than that measured for U) ^{232}Th was measured on a Faraday (although low signal sizes often militate against precise analyses) and ^{238}U was measured by Faraday to quantify any signal fluctuation and used to correct ^{229}Th before calculation of the Daly gain. Details of the performance of the SUERC instrument for a variety of U standards were presented elsewhere by Ellam and Keefe (2006).

Ages of the samples were calculated using the decay constants of Cheng et al. (2000) and Isoplot/Ex rev. 2.49 (Ludwig 2001). The decay constant errors of ^{230}Th and ^{234}U are propagated into the age-error calculation along with errors on the activity ratio to provide overall analytical errors. The effective dating range for U-series dating is considered to be around 6 half-lives of ^{230}Th (~350ka) (Chabaux et al. 2003). However, if an excess of ^{234}U is present, and the initial uranium activity ratio, $(^{234}U/^{238}U)_0$, is adequately high, as is the case in this study, material older than 350ka can be dated.

Item DR2: Repeat Measurements

Repeat analysis was carried out on three samples of distinct age (from mounds L2, L6 and L8) from the Little Grand Wash fault (Table DR1). Considering the small analytical errors on the age results (0.5 to 1%) the repeat analyses demonstrated good levels of reproducibility. The reproducibility in terms of percentage difference between the two repeat analyses was 10.4% for L2, 1.6% for L8 and 6.3% for L6. Recent work utilising U-series dating suggests that the main control on reproducibility is sample integrity rather than analytical capability such that duplicate samples often do not reproduce at the level of precision available from mass spectrometric methods (Thompson 2010). Variation in open-system behaviour of U within the aragonite vein samples is likely to be the main reason for the discrepancies between ages. Samples from the L2 mound provided the least reproducible result as younger samples have low levels of ^{230}Th, leading to inherently poorer counting statistics and increasing any effect from detrital ^{232}Th.

Item DR3: Age Estimates

As dated mound ages correlate with their height above the local drainage we were able to calculate an incision rate for the SWG and use this rate to estimate the ages of non-dated mounds. For this calculation we classed the local drainage as the closest tributary to the Green River and measured elevations using a differential GPS. The height above nearest drainage was determined by subtracting the elevation of the closest section of the tributary from the elevation of river gravel entrained within the dated travertine. These immature piedmont gravels are a key indicator of base level when the travertine was actively precipitated. There are eight dated travertine on the SWG which contain river gravels. Three of these are associated with the Big Bubbling Wash (S7, S8, S9) and five are associated with the Salt Wash (S6, S11, S12, S17, S20) streams. To estimate the ages of non-dated travertine the height of the base of the surface deposited carbonates (or river gravel if present) above the nearest section of local drainage was divided by the calculated incision rate.

Supplemental Figures and Tables

Figure DR1: Geological maps showing the location of U-Th dated travertine (white boxes), from Table S1, and estimated age travertine (green boxes), from Table DR2.

Figure DR2: Images of the Crystal Geyser and associated travertine deposit. A) Picture taken at the peak of geyser activity in the midst of an eruption cycle. B) Close-up of surface carbonate formed by degassing of the run-off water from the geyser. Note the complex morphology of the carbonate and the presence of windblown material from the surroundings. C) SEM image of a surface carbonate sample. The arrows highlight the presence of detrital contamination; grey arrows indicate quartz and the white arrow feldspar.

TABLE DR1: U-TH RESULTS OF TRAVERTINE SAMPLES.

Mound	U-Th age (years) (2σ)	$(^{234}U/^{238}U)_0$ (2σ)	U (ppm)	Th (ppb)	$[^{230}Th/^{232}Th]$
L2.1	5,029 ± 31	5.12 ± 0.01	4.54	0.64	2,875
L2.1▲	8,629 ± 30	4.37 ± 0.01	1.66	730	1.5
L2.2	5,699 ± 26	3.63 ± 0.01	6.49	0.39	50,459
L2.2*	5,060 ± 40	3.65 ± 0.01	5.16	0.24	19,841
L2.2▲	6,927 ± 22	4.67 ± 0.01	3.27	236	11.1
L3.1	50,890 ± 390	4.12 ± 0.02	4.11	1.47	13,721
L3.2	49,088 ± 187	4.42 ± 0.02	2.16	16.37	499
L4	113,912 ± 604	4.01 ± 0.01	5.08	0.04	905,311
L4	109,614 ± 901	5.09 ± 0.01	4.22	0.06	675,748
L4	106,526 ± 544	4.79 ± 0.01	5.09	0.38	888,662
L4	103,172 ± 1,486	4.90 ± 0.02	4.75	§	§
L4▲	114,098 ± 646	3.72 ± 0.01	2.16	63	13.5
L5	31,217 ± 297	5.97 ± 0.03	0.52	13.43	164
L6	61,274 ± 504	6.38 ± 0.02	8.02	0.31	187,559
L6*	56,419 ± 506	6.27 ± 0.02	8.96	0.4	170,636
L7	75,495 ± 656	6.26 ± 0.02	8.3	0.73	93,471
L8	27,405 ± 80	7.23 ± 0.02	5.93	0.64	416,542
L8*	26,716 ± 250	7.42 ± 0.02	7.49	0.08	370,026
S1	38,906 ± 161	2.02 ± 0.01	3.3	0.15	367,166
S2	60,188 ± 443	4.05 ± 0.01	7.31	§	§
S3	29,028 ± 107	4.35 ± 0.01	7.05	0.15	139,424
S4	291,307 ± 5,594	4.18 ± 0.04	3.03	3.54	6,820
S5	413,474 ± 15,127	6.57 ± 0.22	2.41	0.11	212,447
S6	13,068 ± 59	3.34 ± 0.01	6.02	4.74	1,442
S7	100,378 ± 562	5.37 ± 0.01	4.91	0.67	62,991
S8	106,088 ± 660	5.28 ± 0.01	4.75	0.02	168,936
S9	135,135 ± 1,142	5.21 ± 0.02	6.25	0.01	828,531
S10	51,290 ± 248	4.44 ± 0.01	3.2	2.99	5,102
S11	92,792 ± 1,118	4.84 ± 0.02	4.7	0.08	2,217
S12	28,375 ± 238	5.03 ± 0.01	0.79	0.24	11,154
S13	10,797 ± 42	4.91 ± 0.01	3.2	49.25	91
S14	34,971 ± 142	5.31 ± 0.01	4.28	112	44,315
S15	65,085 ± 334	2.84 ± 0.01	2.31	7.5	1,125
S16	57,014 ± 412	5.50 ± 0.01	3.98	13.49	1,871
S17	4,792 ± 30	3.14 ± 0.01	1.7	8.15	89
S18	112,804 ± 634	6.78 ± 0.02	2.39	0.05	462,932
S19	130,666 ± 831	6.75 ± 0.02	2.57	0.36	85,363
S20	110,000 ± 634	6.80 ± 0.02	2.28	0.57	44,284

S21	116,788 ± 691	7.15 ± 0.02	2.14	0.89	28,864
S22	9,749 ± 45	6.96 ± 0.02	2.18	1.8	2,174

▲ Surface carbonate samples.
* Repeat analyses
§ ^{232}Th levels were too low to be counted

For sample location see Figure DR1. Analytical errors are presented as uncertainty in the decay constants (Cheng et al. 2000) propagated to the age uncertainty and are generally 0.5 - 1% of the age. Repeat analyses demonstrate good levels of reproducibility considering the small analytical errors (see MS2). The presence of detrital contamination is shown by the ^{230}Th/^{232}Th activity ratio. Surface carbonate samples have values lower than the limit of 15 to 20 that indicates the presence of non-radiogenic ^{230}Th (Geyh 2008). The addition of thorium from contamination increases the [^{230}Th/^{234}U] and results in an over-calculated age.

TABLE DR2: ESTIMATED TRAVERTINE AGES, DIMENSIONS AND CO_2 CONTENT.

Mound	Age (years)	Area (m^2) ± 1 m^2	Thickness (m) ± 0.1 m	Volume (m^3)	Volume of CO_2 trapped in the mound (tonnes)
LGW (dated)					
L1	71	5,868	1	5,868	7,222
L2.1	5,029 ± 31	240	1	240	295
L2.2	5,380 ± 33	5,122	3.6	5,238	6,447
L3.1	50,890 ± 390	335	1	335	412
L3.2	49,088 ± 187	388	1	388	478
L4	113,912 ± 604	11,610	6	69,660	85,735
L5	31,217 ± 297	2,580	0.6	1,621	1,995
L6	58,847 ± 505	2,043	5	10,213	12,570
L7	75,495 ± 656	72	0.5	36	44
L8	27,067 ± 165	635	2.5	1,588	1,954
SWG (dated)					
S1	38,906 ± 161	471	0.4	188	232
S2	60,188 ± 443	2,229	1	2,229	2,743
S3	29,028 ± 107	634	0.2	150	184
S4	291,307 ± 5,594	332	0.1	41	51
S5	413,474 ± 15,127	1,207	0.4	543	668
S6	13,068 ± 59	1,013	0.5	507	624
S7	100,378 ± 562	833	1	833	1,026
S8	106,088 ± 660	864	0.6	518	638
S9	135,135 ± 1,142	1,110	1	1,110	1,366
S10	51,290 ± 248	199	0.1	15	18
S11	92,792 ± 1,118	5,612	1	5,612	6,907
S12	28,375 ± 238	612	1.2	734	904
S13	10,797 ± 42	911	0.4	364	448
S14	34,971 ± 142	534	0.2	106	131

S15	65,085 ± 334	12,013	0.5	6,006	7,392
S16	57,014 ± 412	2,331	0.6	1,399	1,721
S17	4,792 ± 30	1,080	0.3	324	399
S18	112,804 ± 634	2,614	1	2,545	3,132
S19	130,666 ± 831	4,125	1.5	6,341	7,804
S20	110,000 ± 634	2,392	0.7	1,674	2,061
S21	116,788 ± 691	357	1.1	393	484
S22	9,749 ± 45	637	0.4	255	313
S23	9,342	742	0.5	371	457
SWG (estimated)					
S24	52,942	808	0.3	244	300
S25	13,009	5,230	1	5,230	6,437
S26	58,792	443	0.2	73	90
S27	48,660	651	0.2	158	194
S28	64,336	1,215	0.9	1,094	1,346
S29	690,792	1,013	0.4	383	471
S30	131,934	4,607	0.9	4,146	5,103
S31	82,940	4,236	2	8,472	10,427
S32	162,078	1,896	0.5	948	1,167
S33	190,029	1,124	2	2,248	2,767
S34	320,295	819	0.3	250	308
S35	105,033	819	1	819	1,009
S36	158,825	2,251	0.8	1,888	2,323
S37	77,332	6,296	2.3	14,768	18,177
S38	172,056	1,883	0.7	1,321	1,625
S39	67,375	1,567	0.6	915	1,126
S40	75,919	1,382	0.5	711	875
S41	120,118	1,215	0.5	550	677
SWG (active springs)					
S42	Modern	493	0.2	99	121
S43	Modern	435	0.2	87	107
S44	Modern	3,787	0.5	1,894	2,331
S45	Modern	1,130	0.5	565	695
S46	Modern	1,963	0.2	393	483
S47	Modern	988	0.3	297	365

For travertine locations see Figure DR1. Crystal Geyser (L1) is given an age of 71 years as this was the time between drilling of the abandoned exploration well and the volume estimates. Estimated ages for the SWG mounds use height above the nearest Green River tributary, measured with a differential GPS, divided by the local incision rate of 0.17mm/y.

Additional References

Ellam, R.M. and Keefe, K., 2006, MC-ICP-MS analysis of non-natural U isotope ratios using a $^{229}Th/^{232}Th$ external mass bias correction: Journal of Analytical Atomic Spectrometry, v.22**,** p. 147-152.

Geyh, M.A., 2008, Selection of suitable data sets improves $^{230}Th/U$ dates of dirty material: Geochronometria, v.30, p. 69-77.

Ludwig, K.R., 2001, Isoplot/Ex version 2.49: Berkeley Geochronology Centre Special Publication, v.1[a], 55p.

Thompson, W.G., 2010, Strategies for the treatment of coral age data in the reconstruction of sea-level change, *in* Earth, Energy and the Environment: Proceedings of the 2010 Goldschmidt Conference, Goldschmidt, Knoxville, Tennessee, June 13-18th, 2010.

Yokoyama, T., Makishima, A., and Nakamura, E., 1999, Separation of thorium and uranium from silicate rock samples using two commercial extraction chromatographic resins: Analytical Chemistry, v. 71, p. 135–141.

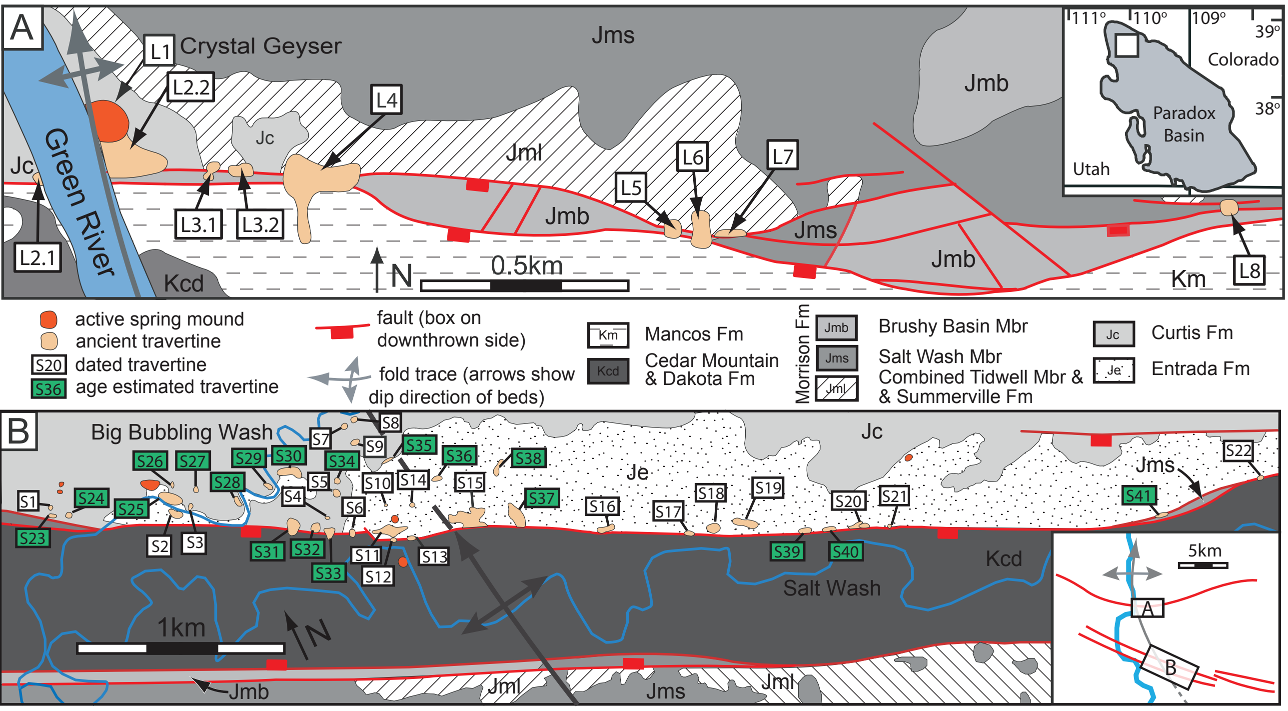
A
Crystal Geyser
Jms
Jmb
Jc
Jml
Green River
L1
L2.2
L2.1
L3.1
L3.2
L4
L5
L6
L7
L8
Kcd
Km
N
0.5km
111°
110°
109°
39°
38°
Colorado
Paradox Basin
Utah
active spring mound
ancient travertine
dated travertine
age estimated travertine
fault (box on downthrown side)
fold trace (arrows show dip direction of beds)
Mancos Fm
Cedar Mountain & Dakota Fm
Morrison Fm
Brushy Basin Mbr
Salt Wash Mbr
Combined Tidwell Mbr & & Summerville Fm
Curtis Fm
Entrada Fm
B
Big Bubbling Wash
Je
Salt Wash
1km
5km
S1 S2 S3 S4 S5 S6 S7 S8 S9 S10 S11 S12 S13 S14 S15 S16 S17 S18 S19 S20 S21 S22
S23 S24 S25 S26 S27 S28 S29 S30 S31 S32 S33 S34 S35 S36 S37 S38 S39 S40 S41

Figure DR1

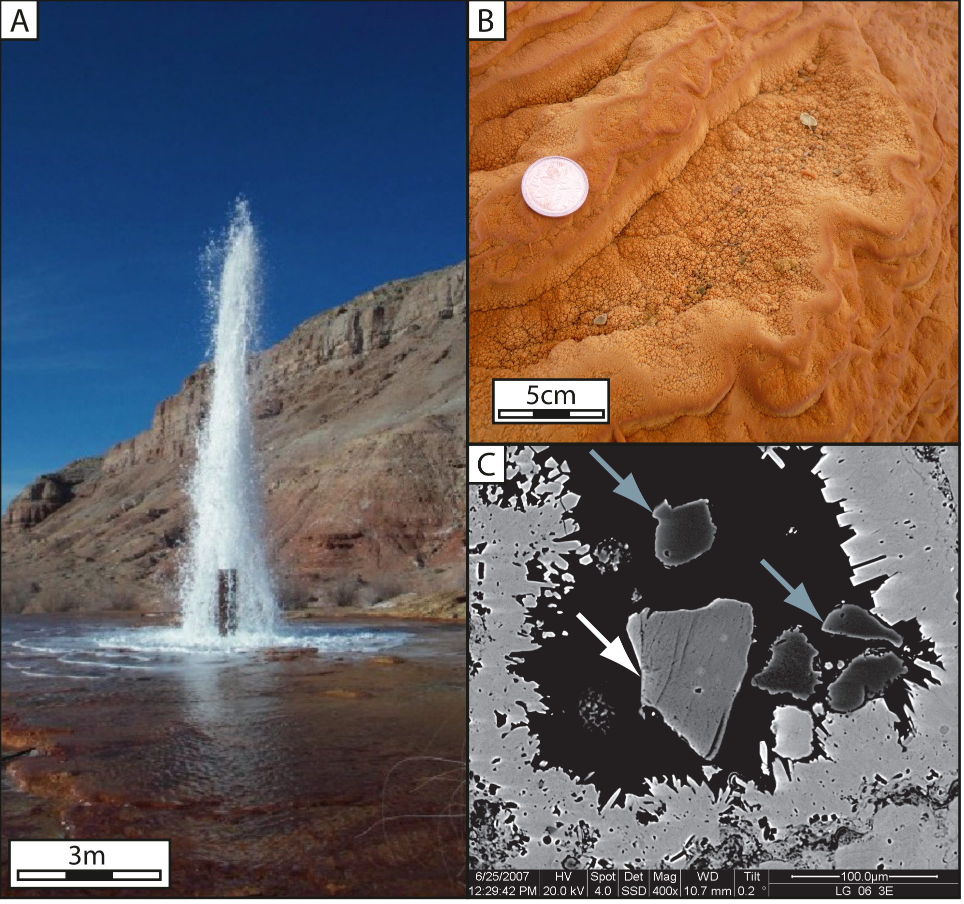
A
3m
B
5cm
C
6/25/2007 12:29:42 PM
HV 20.0 kV
Spot 4.0
Det SSD
Mag 400x
WD 10.7 mm
Tilt 0.2 °
100.0µm
LG 06 3E

Figure DR2